Water Resources Management (2026) 40:117
https://doi.org/10.1007/s11269-025-04368-3

Development of Novel Simplified Empirical Equations for the Estimation of Peak Discharge due to Dam Failures

Rasim Temür[1] · Yasin Paşa[2] · Sezar Gülbaz[3] · İsmail Bilal Peker[3] · Abdülbaki Hacı[2]

Received: 25 June 2025 / Accepted: 12 November 2025
© The Author(s) 2026

Abstract

This study presents a novel methodology for estimating the peak discharge resulting from the failure of earth-fill dams through the development of simplified empirical equations. The proposed method integrates parametric sensitivity analysis, numerical simulations, and meta-heuristic optimization techniques. The historical failure of the Teton Dam in Idaho, USA, was selected as a reference study area due to the availability of reliable spatial and hydraulic data, and the developed models are therefore mainly applicable to piping-type failures in earth-fill dams. Five critical parameters were initially considered in the dam breach analysis: bottom breach width (*BBW*), breach side slope (*SS*), breach development time (*BDT*), volume of water above breach invert (V_w), and water height at piping initiation (H_w). A total of 2000 dam failure scenarios were simulated using the Hydrologic Engineering Center's – River Analysis System (HEC-RAS), and the results were analyzed to derive empirical models. Correlation analysis revealed that while *BBW* and *BDT* have strong correlation with Peak Breach Flow (Q_p) and clear directional influence, *SS* had a minor direct effect. In contrast, H_w and V_w exhibited complex and nonlinear behavior due to their interdependence with *BDT*. Although they physically affect Q_p, their influence is non-monotonic and scenario-dependent. For empirical equation development approach, their contribution was found to be minimal compared to *BBW* and *BDT*. As a result, simplified empirical equations were developed using the most influential parameters. Multiple empirical equation structures were investigated: (i) single-parameter models, (ii) two- and three-parameter models, and (iii) a novel table-driven model where the coefficients adapt dynamically based on discrete values of the third parameter. Among these, the table-driven empirical equations performed the best, with a maximum absolute percent error ranging from 20.3% to 25.1%, significantly improving the accuracy compared to fixed-coefficient models. Coefficients of the empirical models were optimized using the Teaching–Learning-Based Optimization (TLBO) algorithm, which proved effective in calibrating the nonlinear relationships between breach parameters and peak flow. The proposed empirical equation family, named Simplified Empirical Equation for Dam failure (SEED), provides a rapid and flexible estimation framework that can support early warning systems, dam breach risk assessment, and emergency action planning. The study demonstrates that well-designed empirical equations, when supported by robust simulation and optimization techniques, can offer reliable approximations for complex dam breach hydraulics, especially in data-scarce or time-critical scenarios.

Extended author information available on the last page of the article

Published online: 12 February 2026

Keywords Dam breach modeling · Empirical equation · HEC-RAS simulation · Peak discharge estimation · Meta-heuristic and teaching–learning-based optimization (TLBO) · Teton dam

1 Introduction

Dams are important structures for the economy of the country and provide the need for continuous water supply, which is essential for human life (Chen et al. 2015; Zhu et al. 2021; Dai et al. 2025). However, the volume of water stored in a dam always poses a risk to the downstream part of the dam (Wang et al. 2024; Moreno-Rodenas et al. 2025). The flood wave, which is caused by the dam collapse and spreads rapidly in the downstream direction, can cause the release of large amounts of water, serious material damage, and loss of life (Galoie et al. 2012; Macchione et al. 2015; Ge et al. 2022; Baird et al. 2024). The magnitude of the flood wave, typically resulting from dam failure, is greater than that of other types of floods, such as river or coastal floods. The time to reach peak flow is also shorter, and the time available for warning and evacuation of residents living downstream of the dam is significantly limited (Paşa et al. 2023; Peng et al. 2024). Effective risk management efforts are crucial to reduce the structural vulnerability of critical infrastructures such as dams and prevent damage (Nasser et al. 2025).

Dam failure is recognized as one of the most devastating disasters in terms of the number of casualties and economic losses (Foster et al. 2000; Altinbilek 2002; Sanchez-Mondragon et al. 2023; Liu et al. 2024), as well as its negative socio-economic and ecohydrological impacts (He et al. 2020; Zhang et al. 2022a). The analysis of studies that could result in catastrophic disasters such as dam failures is vital for humanity and nature. Therefore, it is crucial to ensure the safety and reliability of dams through proper maintenance, monitoring and risk assessment (Peng and Zhang 2013; Zamarrón-Mieza et al. 2017). The fact that most dams in the world have reached their structural lifespan and the increase in extreme weather events due to climate change brings the issue of dam failures to the agenda (Fluixá-Sanmartín et al. 2018; Stamou et al. 2025). In recent years, researchers have been evaluating the conditions of dams in different regions of the world to determine their potential for failure (Costa and Schuster 1988; Lyu et al. 2019; Nasser et al. 2025). In such a significant issue, it is important to analyze hydraulic indicators aimed at estimating the severity of damage, such as peak flowrate or flood depth. Especially in the downstream regions of old and large dams, a robust mathematical expression of this physical phenomenon is needed for an estimation such as peak flowrate in flood scenario simulations that may occur as a result of any possible collapse (Xu et al. 2012; Qiu et al. 2024).

In dam failure studies, computer programs are preferred as a practical method to determine the dimensions of the disaster (Bharath et al. 2021). Various dam failure simulation softwares are used in different parts of the world (Kumar et al. 2017). All modeling programs developed for dam failure analyses operate with empirical equations of physical phenomena regardless of the software type. These equations are embedded in computer software such as DAMBRK (Fread 1984), MIKE (DHI 2017), and HEC-RAS (USACE 2016). Numerous empirical equations were developed to incorporate certain physically based geometrical characteristics and the temporal evolution of the breach formation during dam failure simulations (MacDonald Thomas and Langridge-Monopolis 1984; Von Thun and Gillette 1990;

Froehlich 1995a, 2008; Xu and Zhang 2009). Furthermore, empirical equations defined with different parameters and coefficients were derived to determine the peak flood flowrate that historical dam failure events by many researchers (Kirkpatrick 1977; SCS 1981; Hagen 1982; USBR 1982; MacDonald Thomas and Langridge-Monopolis 1984; Singh and Snorrason 1984; Costa 1985; Evans 1986; Froehlich 1995b; Walder and O'Connor 1997; Xu and Zhang 2009). These equations have their own limitations and assumptions due to their development with limited datasets for smaller dams mostly, and the accuracy of the estimated peak flowrate may depend on the specific conditions of the dam and its watershed. To achieve a more robust estimate of the potential impact of a dam failure, applying multiple equations and comparing the results is effective (Shourian et al. 2007; Macchione et al. 2015). Also, it is important to note that empirical equations provide only rough estimates of peak flowrates and should be used with caution. Actual peak flows may vary significantly depending on a variety of factors, such as the size and shape of the reservoir, the volume and velocity of the water released, and the topography of the downstream area (Wahl 1998; Brunner 2014; Haltas et al. 2016). Recent studies show that reservoir side slopes can greatly affect flood size and timing (Hooshyaripor and Tahershamsi 2015).

Most dam failures are initiated by the formation of a breach, although the causes can differ (Xiong 2011). To estimate the peak flowrate resulting from dam failure, it is essential to define certain factors, such as breach geometry (bottom width or side slope) and breach formation time. Moreover, the estimation of the peak flowrate after the breach progression, the factors such as flow conditions and dam type should be affected (Brunner 2014). These geometric and flow-related physical conditions have been parameterized in the aforementioned empirical equations used to describe dam failure. However, each empirical equation differs due to the number of parameters and the failure types it represents. For example, Xu and Zhang (2009) estimated the peak flowrate resulting from dam failure with six different parameters related to the geometry of the dam body, water volume in the dam reservoir and failure mode. On the other hand, the equation proposed by Froehlich (1995b) defines only two parameters related to the height and volume of water in the reservoir. In recent years, several studies have attempted to refine empirical equations and enhance the understanding of dam breach parameters (Dhiman and Patra 2019; Zhong et al. 2020; Azmi and Thomson 2024; Marangoz et al. 2024). Accordingly, comprehensive empirical equations are required that can represent different types of dams and failure modes that transform physical phenomena into mathematical expressions in dam failure analysis.

The current literature presents linear equations for estimating the peak discharge of dam break hydrographs. Nevertheless, these generalized equations are considered inadequate for accurately capturing the complexity of the phenomenon and the interactions between parameters due to their highly generalized nature. To overcome this limitation, this study derives novel empirical equations for estimating the peak flood flowrate from breaching failure of an earth-fill gravity dam. To derive these equations, this study conducted an analysis of 2000 scenarios comprising various combinations of breach development time (*BDT*), breach side slope (*SS*), water height at piping initiation (H_w), volume of water above breach invert (V_w), and bottom breach width (*BBW*) parameters. These scenarios were developed based on the physical characteristics of the Teton Dam, an earth-fill dam which collapsed in Idaho, USA, in 1976. Extensive scientific studies were carried out on this dam, and the scenarios were modelled using the HEC-RAS software. The results demonstrate that different parameter combinations produce varying impacts on the peak discharge. The fundamen-

tal contribution of this work is the establishment of a differentiated set of equations. This approach significantly reduces the potential for high error percentages, inherent in using a single generalized equation, by systematically classifying the behavioral shifts of parameters within specific ranges. This equation (SEED) can also serve as a guideline for the peak flood flowrate estimation for the earth-fill dams.

2 Materials and Methods

2.1 Study Area: Teton Dam Failure

Teton Dam was located on the Teton River, 4.83 km northeast of Newdale, Idaho, United States of America (Fig. 1), and it was constructed by the Bureau of Reclamation in 1975 (Barnes 1992). The Teton River flows from the western side of the Teton Mountains and the northeastern side of the Big Hole Mountains, which are situated on the border of Idaho and Wyoming. Teton Dam was constructed in a narrow canyon with steep walls that were formed by the Teton River. The Teton Canyon finishes about 8.05 km past the dam (Gra-

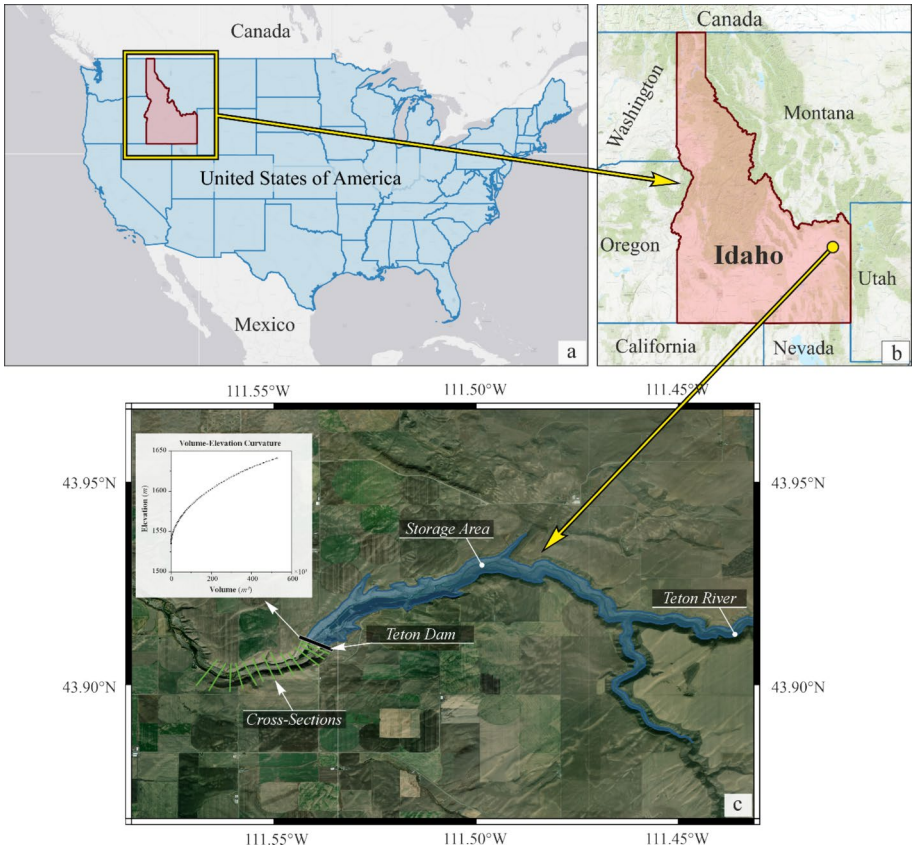


Fig. 1 Location of Teton Dam, 1-D model cross-sections, storage area, layout of the dam body, and volume-elevation curvature. (Source of the basemaps: **a**. ESRI (2025a); **b**. ESRI (2025b); **c**. ESRI (2025c))

ham 2008). Teton Dam was a zoned earth-fill dam with a body height of 93 m above the river bed, and a crest length of 945 m. The drainage area of Teton Dam was 2,210 km^2. The primary purpose of this dam was flood control, hydropower, recreation, and irrigation (Chadwick et al. 1976). Detailed properties of Teton Dam are presented in Table 1. Internal erosion (piping) started at Teton Dam when the reservoir water level reached 1,616 m elevation, which was 6.89 m lower than the highest water level and 1.01 m below the spillway threshold (Chadwick et al. 1976). Based on the dam's structural height, the Teton Dam failure was the largest embankment failure in the USA. The inundation area extended to 777 km^2 and reached up to 129 km downstream, where areas were fully or partially inundated (Snorteland 2009). According to the report of an independent panel to review the cause of the Teton Dam failure, 14 people died and estimated property damage was between 400 million to one billion dollars (Chadwick et al. 1976). Because of the availability to have observed data and a digital elevation model, this case study was selected for simulations.

2.2 HEC-RAS Model Setup

The HEC-RAS calculates the flow at piping or overtopping type dam breaks using the orifice and weir equations. When the dimensions of the piping are sufficiently large, the weight of the material situated above the piping zone exceeds the capacity of the area where the piping hole is formed, leading to a collapse. This collapse accelerates the breaching process. At this stage, the flow transitions from pressurized (orifice-type) flow to weir-type flow (USACE 2020). The full flowing orifice equation and the weir equation are presented as Eqs. 1 and 2, respectively.

$$Q = C \cdot A \cdot \sqrt{2 \cdot g \cdot H} \tag{1}$$

where, Q is total flow over the weir, H is the difference between the energy gradient elevation upstream and the water surface elevation downstream, A is net area of openning and C is coefficient of discharge for fully submerged pressure flow. Typical value of C is 0.8.

$$Q = C \cdot L \cdot H^{3/2} \tag{2}$$

where, Q is total flow over the weir, C is coefficients of discharge for weir flow, L is effective length of the weir, H is difference between energy upstream and road crest.

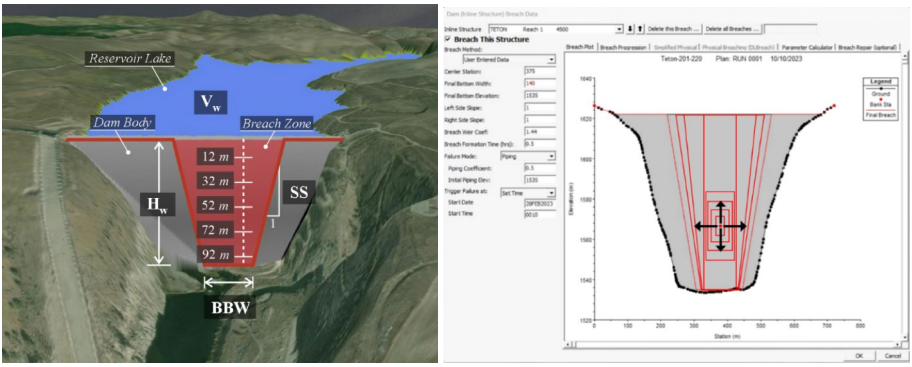
Table 1 Properties of Teton Dam (Zhang et al. 2022b)

	Teton Dam
Dam type	Zoned earth-fill
Spillway type	Gated chute spillway
Dam height	123.4 m
Crest elevation	1,625 m
Maximum water surface elevation	1,622.8 m
Crest length	945 m
Crest width	10.7 m
Upstream side slope	2.5: 1
Downstream side slope	2: 1

The breach model of the Teton Dam was developed using HEC-RAS. The topographic characteristics of the study area were defined using a digital elevation model (DEM) of the region. For this purpose, the National Elevation Dataset (NED) (Gesch et al. 2002), with a spatial resolution of 3 × 3 m and provided by the United States Geological Survey (USGS), was utilized. The volume-elevation curve derived from the NED-based topographic data was used as an input to the HEC-RAS model (Fig. 1). The outflow resulting from the dam break scenarios (Piping) was incorporated into the 1-D model by discharging it through the defined cross-sections. The dam body was represented as an inline structure, and the dam characteristics listed in Table 1 were incorporated into the model. A three-dimensional visualization of the dam body, reservoir, and spillway configuration is shown in Fig. 2a, while a screenshot of the dam failure module in HEC-RAS is provided in Fig. 2b.

2.3 Scenarios

Several parameters influence the peak discharge resulting from dam breaches. These parameters are breach development time (*BDT*), breach bottom width (*BBW*), breach side slope (*SS*), and water height at piping initiation (H_w). Besides these, another parameter that is influential, V_w, varies depending on H_w and can be determined based on its values. The parameter ranges of *BBW*, H_w, V_w were defined based on the physical characteristics of the Teton Dam since this study focuses on that specific dam. On the other hand, the parameter ranges for the *SS* and *BDT* parameters are based on the dataset established by Xu and Zhang (2009), which was compiled from an analysis of 75 dam failure cases featuring critical measurements. Accordingly, for this study, the *BDT* parameter was selected within the range of 0.5–5.0, and the *SS* parameter within the range of 0.4–1.0. As illustrated in Fig. 3, ten time intervals ranging from 0.5 to 5 h with 30-min increments were defined for *BDT*. For *BBW*, ten values between 20 and 200 m were selected in 20-m increments. For *SS*, four slope values between 0.4 and 1.0 were used in 0.2 increments. Finally, for H_w, five breach heights were chosen, ranging from 12 to 92 m, with 20-m increments.



(a) (b)

Fig. 2 The parameters such as *BBW*, *SS*, H_w, *and* V_w used in the empirical equation shown on the **a** schematic of Teton Dam body, and **b** the piping-type breach development pattern in HEC-RAS dam failure module. (Source of the basemap: Google Earth Pro (2025))

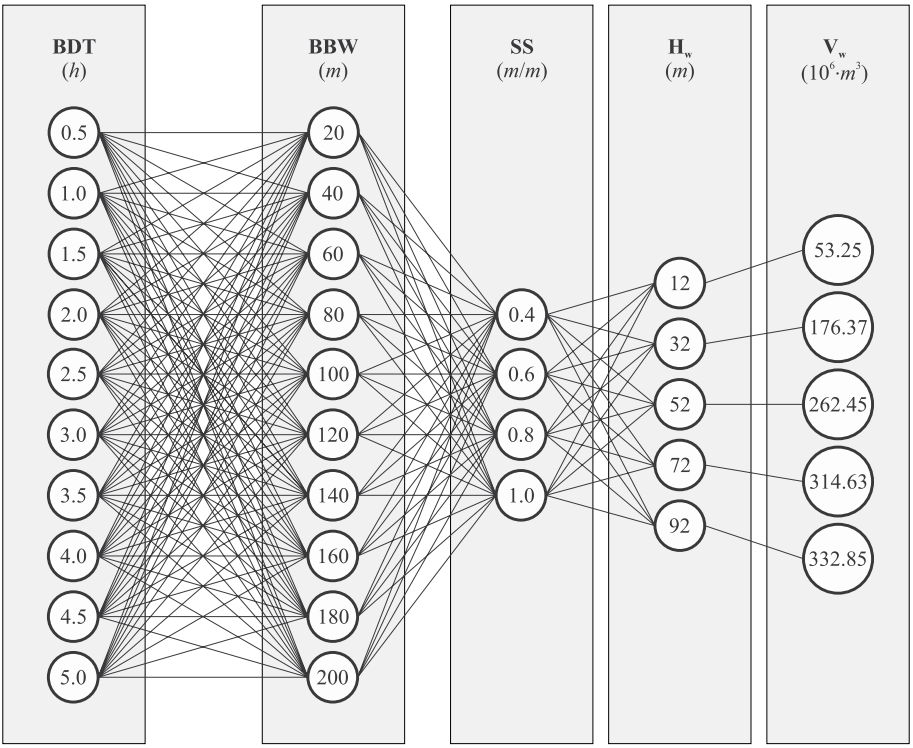


Fig. 3 Numerical values and configurations used in the scenarios

Based on these ranges, 2,000 scenarios (10 of BDT × 10 of BBW × 4 of SS × 5 of H_w and V_w) were generated and simulated using the HEC-RAS. The selected ranges and number of divisions for each parameter were determined to enable a comprehensive examination of both lower and upper bounds, as well as to evaluate various intermediate conditions. Additionally, the piping coefficient was set to 0.5 for all breach scenarios, based on the coefficient table recommended by USACE (2020).

2.4 Empirical Equation Development

As explained in the previous section, the structure of the empirical equation is developed to estimate the peak discharge from a dam failure. The flow chart of the empirical equation derived is shown in Fig. 4. The suggested empirical equation is as follows:

$$Q_p = CC \cdot \frac{BBW^a \cdot SS^b \cdot {V_w}^c \cdot {H_w}^d}{BDT^e} \tag{3}$$

where a, b, c, d, e are the empirical coefficients, CC is the correction coefficient. BBW is the bottom breach width (L), SS is the breach side slope (m/m), BDT is the breach development time (T), V_w is the volume of water stored above breach invert (L^3), and H_w is the water height at piping initiation (L). The correction coefficient and the empirical coefficients

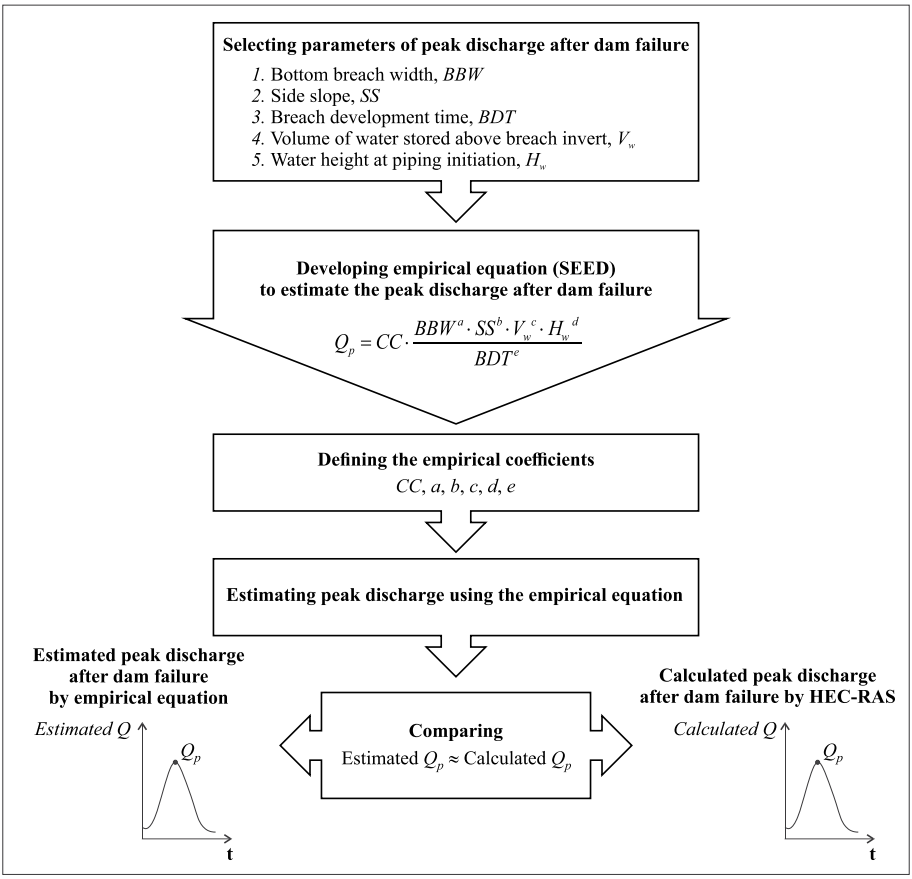


Fig. 4 Empirical equation flow chart for peak discharge after dam failure

are determined using an optimization algorithm. The difference between the calculated and estimated values is minimized using these algorithms. Thus, determination of the correction and empirical coefficients can be considered as an optimization problem.

An objective function must be defined in optimization methods to obtain optimum values. In this study, the objective function is defined as follows:

Minimize: $f(x) = \%_{error}, x = (a, b, c, d, e)$

$$\%_{error}(i) = \left| \frac{Q_p^{estimated}(i) - Q_p^{calculated}(i)}{Q_p^{calculated}(i)} \right| \cdot 100, 1 \leq i \leq nd \tag{4}$$

where $Q_p^{estimated}$ and $Q_p^{calculated}$ are the estimated and calculated peak discharge, respectively, $\%_{error}$ is the absolute peak error between estimated and calculated peak discharge, *nd* is number of peak discharge data.

2.5 Optimization Method

The empirical equation template (Eq. 3) presented in Sect. 2.3, called "Simplified Empirical Equation for Dam Failure" (SEED), considers five different parameters that are effective in dam failure. The equation includes six coefficients, consisting of an exponential term for each parameter (a, b, c, d, and e) and a constant multiplier (CC).

In a similar study by Gulbaz et al. (2019), it was presented that the meta-heuristic approach can produce appropriate solutions in the calibration of empirical equations of this type. In this study, considering the number of coefficients and the nature of the problem, the same approach will be employed for the calibration of coefficients in this equation form. Although numerous heuristic algorithms exist in the literature, many of them require problem-specific parameter calibration due to their dependence on algorithm-specific parameters. In this study, the Teaching–Learning-Based Optimization Algorithm (TLBO), developed by Rao et al. (2011), will be employed. TLBO has been widely used in various engineering problems, providing reliable and consistent results without requiring algorithm-specific parameters.

TLBO, which mimics the learning process within a classroom, begins by randomly generating an initial solution set, similar to other heuristic algorithms. It then operates in two distinct phases, each governed by its own solution-update equations. The flow chart of the TLBO algorithm is illustrated in Fig. 5.

In this study, the objective function is to minimize the maximum absolute peak error between the peak discharge values in the dataset and those obtained from the optimized equation. The optimized equation is run for all scenarios in the dataset and discharge values are obtained. The peak error is then estimated by comparing these values with the calculated peak discharge values in the dataset. The absolute values of the obtained error rates are taken, and the maximum error rate is identified.

In the preliminary analyses conducted to adapt the meta-heuristic algorithm to the problem showed that 20 populations and 10,000 iterations are sufficient to obtain reliable results for the current data size and problem type. These values were also used in the algorithm for the calibration of the empirical equation parameters. Stopping criterion is defined as the maximum number of iterations. The T_F parameter is randomly set to 1 or 2, as specified by Rao et al. (2011). The k parameter in the flow chart is a loop variable used to work with the population size.

3 Results and Discussion

The empirical equation template in Eq. 3 was calibrated using the meta-heuristic optimization algorithm described in Section 2.4. The CC parameter was not defined with lower and upper bounds. The condition that the exponential parameters to be calibrated (a, b, c, d, and e) must be positive was defined in the algorithm. The purpose of this definition is to obtain results that are compatible with the equation template. Accordingly, the lower bound of these parameters was constrained to zero, whereas no upper bound was specified. Each empirical equation configuration was independently optimized ten times to ensure that the values obtained as a result of the optimization process are not local minima. The minimum value obtained from the independent optimization processes was accepted as the final result and is presented in the following sections.

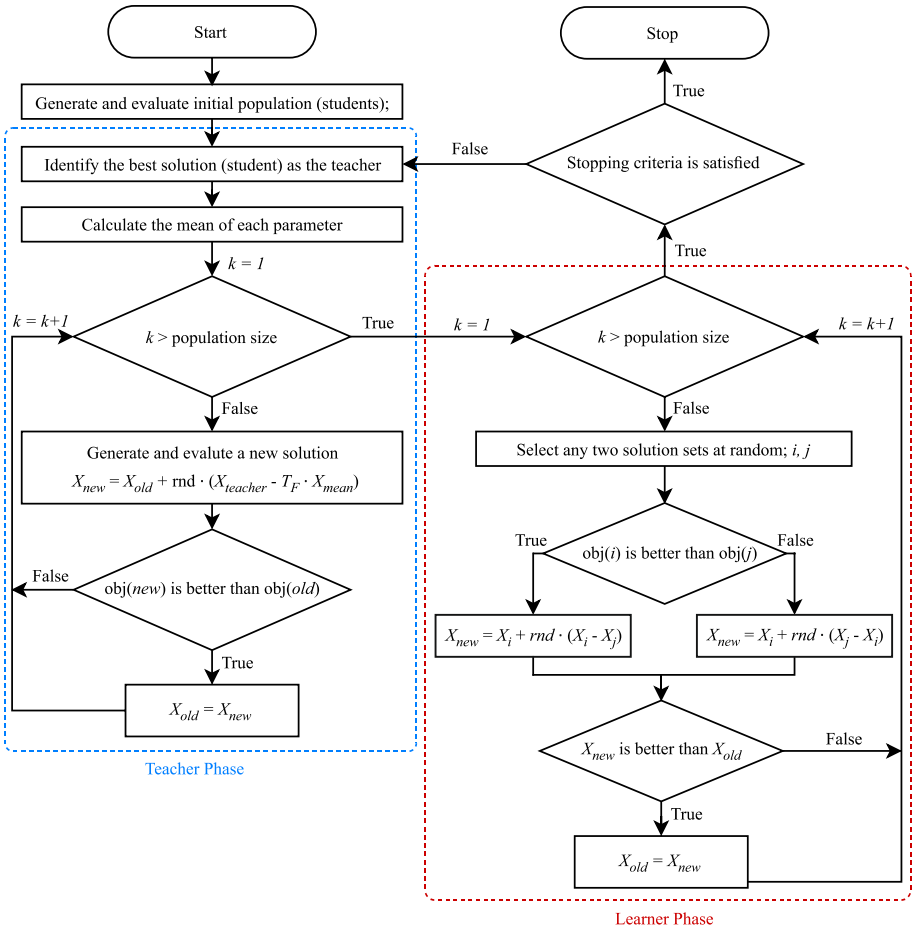


Fig. 5 Flow chart of the meta-heuristic optimization algorithm TLBO

3.1 The Single-parameter Equations

The optimization results and absolute peak error rates of the single-parameter empirical equation forms are provided in Table 2. The abbreviations indicate the number of parameters included for each SEED and the number of the equation. Accordingly, for single-parameter equations, the first equation is *BBW*, the second is *BDT*, the third is *SS*, the fourth

Table 2 Empirical equations with single-parameter

Name	Equation	Max $\%_{error}$
SEED-PI-1	$Qp = 9945 \cdot BBW^{0.38}$	67.6%
SEED-PI-2	$Qp = \frac{60186}{BDT^{0.39}}$	65.7%
SEED-PI-3	$Qp = 47855 \cdot SS^{0.16}$	79.6%
SEED-PI-4	$Qp = 41843 \cdot {H_w}^0$	81.8%
SEED-PI-5	$Qp = 41843 \cdot {V_w}^0$	81.8%

is H_w, and the fifth is V_w. For example, the abbreviation SEED-PI-1 refers to the equation generated using the one-parameter approach in SEED, specifically the first numbered parameter (*BBW*).

In the single-parameter optimized equations, the minimum $\%_{error}$ is 65.7% for the SEED-PI-2 equation using the *BDT* parameter, while the error rates for *BBW*, *SS*, H_w, and V_w are 67.6%, 79.6%, 81.8%, and 81.8%, respectively.

The scatter plots presented in Fig. 6, corresponding to the single-parameter equations optimized using the template equation, reveal that these empirical equations produce a limited number of different values. Furthermore, the obtained peak discharge estimates are limited to a relatively narrow range compared to the calculated peak discharge values.

During the optimization of equations involving the parameters H_w and V_w, the resulting exponential coefficients were found to be zero. According to the defined equation form, this indicates that these parameters do not influence the outcome. Therefore, it is necessary to investigate the effect of these parameters on the peak discharge. For this purpose, a correlation matrix was calculated to analyze the relationships among *BBW*, *BDT*, *SS*, H_w, V_w, and Q_p values in two thousand scenarios obtained by numerical analysis. The Pearson Correlation Coefficient method was employed in this analysis, and the resulting values are presented in Fig. 7.

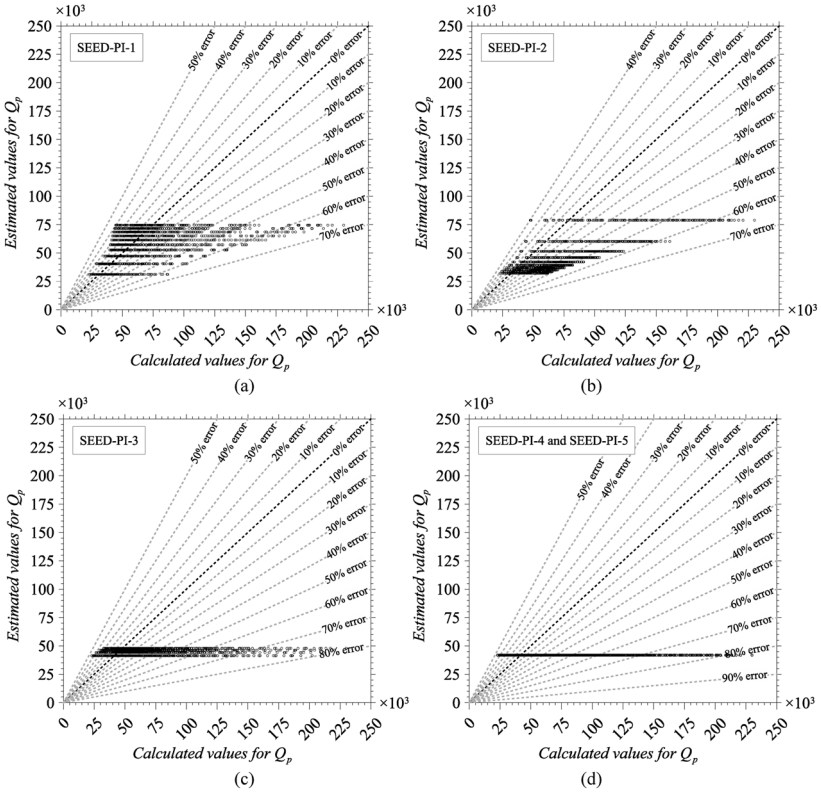


Fig. 6 Scatter plots of empirical equations with single-parameter

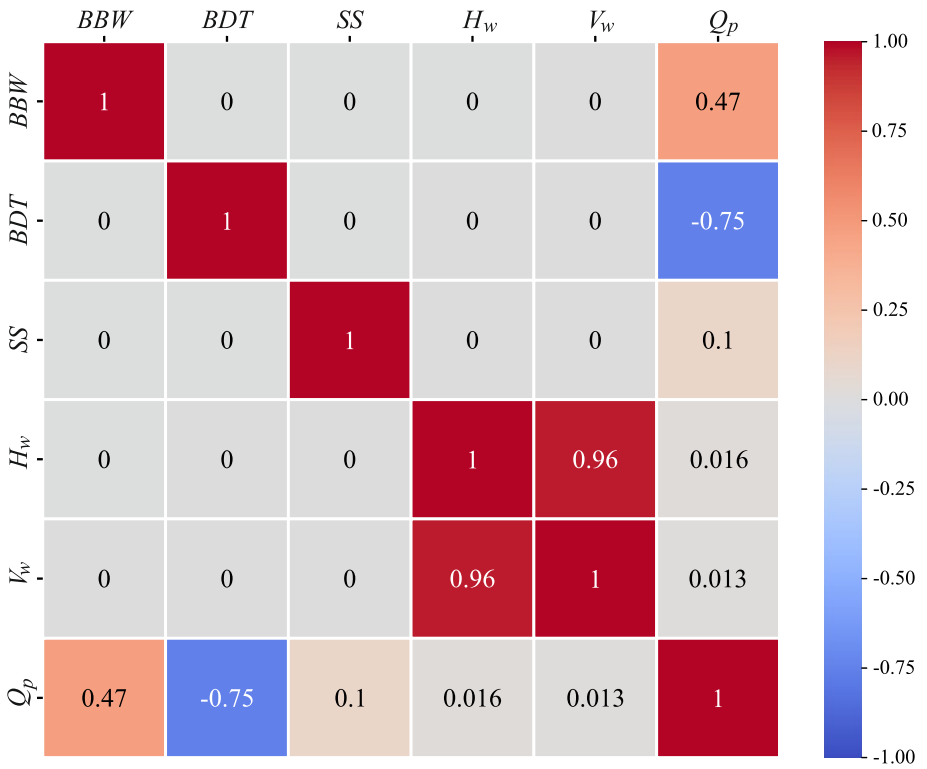


Fig. 7 Correlation matrix of the parameters

In this matrix, where the correlation relationship between the parameters is expressed with values between –1 and + 1. Positive values denote a direct proportional relationship, whereas negative values signify an inverse proportional relationship. A correlation coefficient close to zero implies a weak relationship between parameters, while values further from zero suggest a stronger correlation. The correlation coefficients of *BBW*, *BDT*, and *SS* with Q_p are 0.47, –0.75, and 0.1, respectively. According to these values, *BBW* is directly proportional to Q_p; a wider breach allows for greater water outflow in a shorter time. *BDT*, representing the time it takes for the breach to develop, shows a strong inverse relationship with Q_p. A longer breach development time leads to attenuation of the peak discharge, due to a more gradual release of water from the reservoir. The breach side slope (*SS*) had a minor positive correlation with Q_p.

On the other hand, H_w and V_w presented a more nuanced interaction. These two parameters are physically and mathematically interdependent (The correlation value with each other is 0.96, see Fig. 7): as H_w increases, V_w also increases. However, the influence of these parameters on Q_p is nonlinear and context-dependent. Detailed analysis of model results under various configurations revealed that the relationship between H_w (and thus V_w) and Q_p is not monotonic (Fig. 8). At low *BDT* values (e.g., 0.5 h), increasing H_w from 12 to 52 m leads to an increase in Q_p, as the higher head produces greater driving energy and larger reservoir volume enhances flow capacity. Yet beyond 52 m (e.g., at H_w = 72 m and 92 m), Q_p begins to decrease. This counterintuitive behavior is due to the way HEC-RAS simulates piping-type dam failures: breach development takes time, and during this time, the reservoir

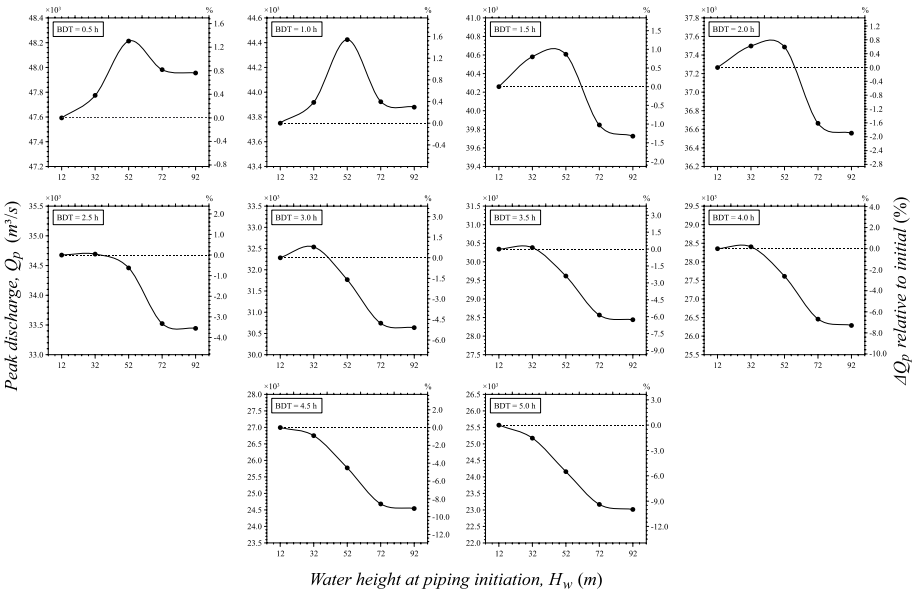


Fig. 8 Change in the water height at piping initiation – the peak discharge (H_w–Q_p) relationship for different values of breach development time (*BDT*)

begins to drain. When the piping initiates too deep (i.e., H_w is large), the breach takes longer to reach the water surface, and a significant portion of the reservoir volume is released at lower flowrates over a prolonged duration, reducing the peak discharge.

This attenuation effect becomes even more pronounced at higher *BDT* values (e.g., 5 h), where the breach develops slowly, allowing even more time for the flood wave to dissipate. In such cases, the relationship between H_w/V_w and Q_p becomes inversely proportional. Thus, while a larger volume exists behind the dam, the flow is not instantaneous, and the peak is subdued.

Although H_w and *Vw* clearly influence Q_p in a nonlinear and *BDT*-dependent manner (Fig. 8), their contribution to the empirical equation approach was minimal. Their non-monotonic behavior complicated coefficient calibration, and thus they were not retained in the final simplified model. The equation template was then revised to include only three parameters, as shown in Eq. 5.

$$Qp = CC \cdot \frac{BBW^{a} \cdot SS^{b}}{BDT^{c}} \tag{5}$$

3.2 The Two-parameters Equations

Three different configurations of the revised equation template with two parameters were also calibrated to be used when all three parameters are not available and the results are presented in Table 3. Among these, the equation named SEED-PII-1, which includes the *BBW* and *BDT* parameters, yielded a maximum absolute peak error of 37.2%. However, the equations SEED-PII-2 and SEED-PII-3, both of which include the *SS* parameter, produced

Table 3 Empirical equations with two-parameters

Name	Equation	Max $\%_{error}$
SEED-PII-1	$Qp = 17582 \cdot \frac{BBW^{0.35}}{BDT^{0.38}}$	37.2%
SEED-PII-2	$Qp = 15549 \cdot BBW^{0.30} \cdot SS^{0.1}$	66.9%
SEED-PII-3	$Qp = 92569 \cdot \frac{SS^{0.48}}{BDT^{0.37}}$	61.9%

peak discharge estimates with significantly higher maximum absolute peak error of 66.9% and 61.9%, respectively. The substantially higher error rate associated with the equations involving the *SS* parameter can be attributed to its relatively weak correlation with Q_p compared to *BBW* and *BDT*.

The graphs of the two-parameter equations optimized in this study show that the SEED-PII-1 equation using *BBW* and *BDT* parameters can produce values with a wider range and lower error rate than the other two-parameter equations. This can be attributed to the stronger correlation of *BBW* and *BDT* with Q_p relative to the *SS* parameter (Fig. 9).

3.3 The Three-parameters Equation

The revised equation template (Eq. 5) was finally calibrated, considering all three parameters (*BBW*, *BDT*, and *SS*). The coefficients presented in Table 4 and absolute peak error rate

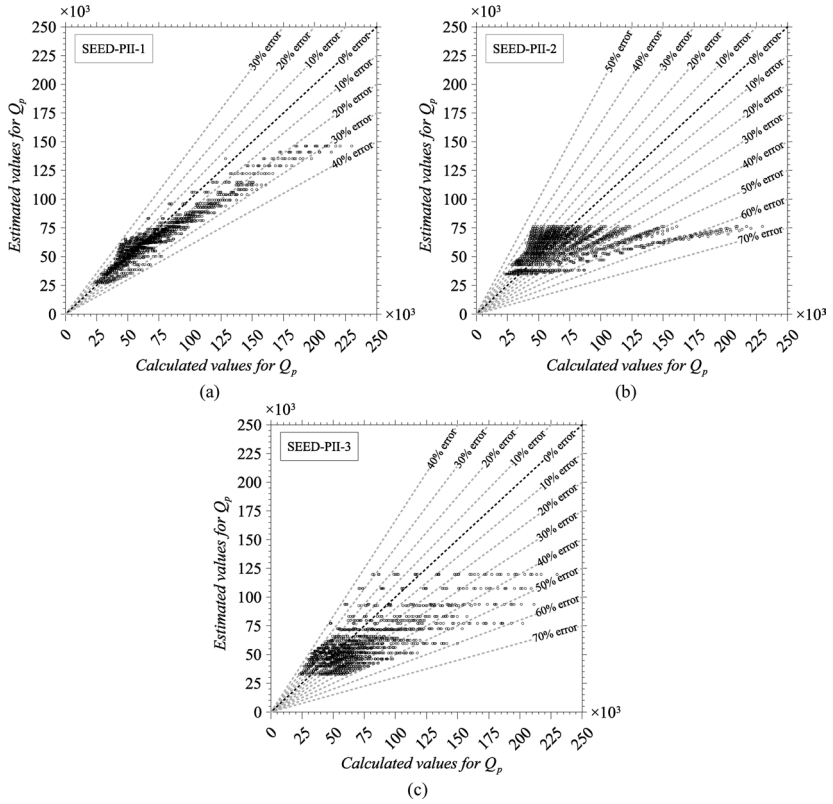


Fig. 9 Scatter plots of empirical equations with two-parameters

Table 4 Empirical equation with three-parameters

Name	Equation	Max $\%_{error}$
SEED-PIII	$Qp = 20159 \cdot \frac{BBW^{0.35} \cdot SS^{0.26}}{BDT^{0.47}}$	32.3%

of 32.3% were obtained for SEED-PIII. This error rate is slightly lower than, but comparable to, that of the two-parameter SEED-PII-1 equation. An examination of the scatter plot of Q_p values generated using this equation, shown in Fig. 10, reveals a better distribution compared to all previously discussed equations. Furthermore, the distribution pattern of the SEED-PIII equation closely resembles that of SEED-PII-1, as also observed in the figure.

All of the empirical equations optimized and analyzed above were designed to estimate peak discharge (Q_p) using a single equation. However, using a single equation with fixed coefficients for the entire dataset may not adequately capture potential nonlinear interactions among the parameters. To address this limitation, a set of alternative equations was developed in which two of the parameters were included, while the coefficients varied depending on the specific value of the third parameter.

In the dataset used in this study, the *BBW* and *BDT* parameters each take 10 different values, while *SS* assumes 4 distinct values (see Fig. 3). Accordingly, for each possible value of these parameters, multiple equations were generated involving the remaining

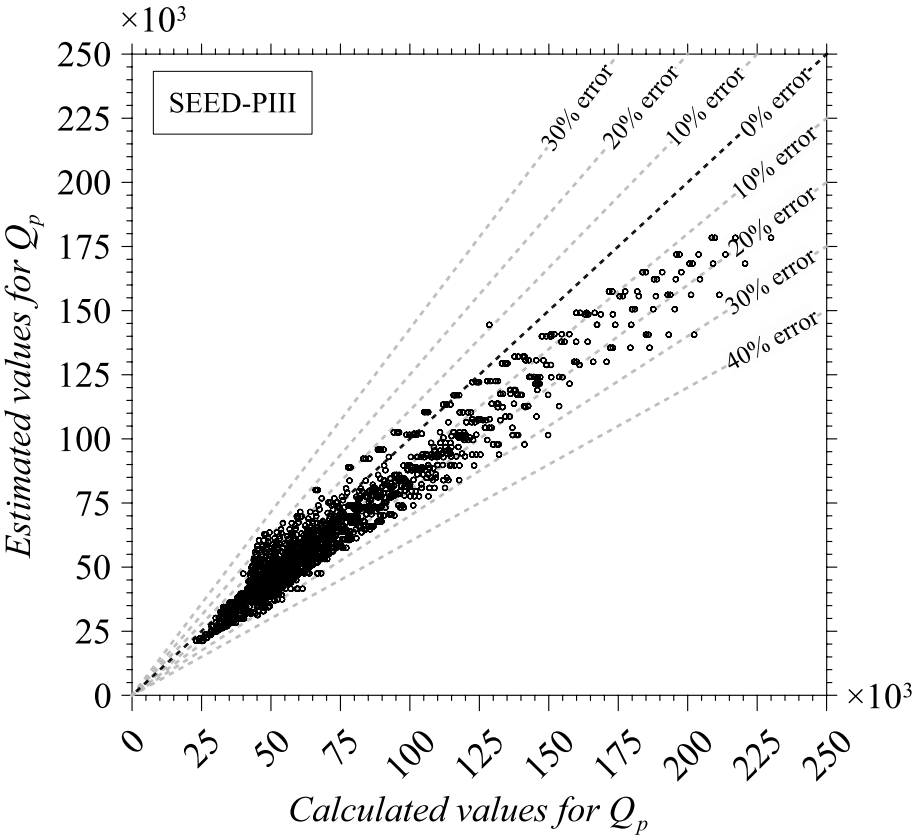


Fig. 10 Scatter plots of empirical equation with three-parameters

two parameters, but with varying coefficients. Although these equations contain only two parameters, the coefficients are selected from predefined tables based on the value of the third parameter.

3.4 The Table-driven Equation Approach

To take into account nonlinear interactions between parameters, a table-driven approach was examined. The optimized equations derived through this table-driven equation approach, along with their corresponding coefficients and maximum error rates, are presented in Table 5. Based on these results, the equations generated according to different values of *BBW*, *BDT*, and *SS* produced maximum absolute error rates of 20.3%, 21.4%, and 25.1%, respectively. These values are considerably lower than the 32.3% error rate obtained with the single empirical equation models.

As shown in the scatter plot in Fig. 11, the distribution of Q_p values produced by the table-driven equation approach is comparable to that of the three-parameter single empirical equation. Among the table-driven equation models, the SEED-SS equation based on fixed *SS* values produced the highest maximum error. This is consistent with earlier findings and is due to the relatively weak correlation between *SS* and Q_p.

This study introduces a novel methodology for developing simplified empirical equations (SEED) to estimate peak discharge in the event of earth-fill dam failure, with a specific focus

Table 5 Table-driven empirical equations and their parameters

Name	Equation	Constant value	*CC*	*a*	*b*	$\%_{error}$*	Max $\%_{error}$
SEED-BBW	$Qp = CC \cdot \frac{SS^{a}}{BDT^{b}}$	BBW = 20	67824	0.52	0.37	14.5%	20.3%
		BBW = 40	74336	0.31	0.43	14.1%	
		BBW = 60	82435	0.15	0.38	14.5%	
		BBW = 80	97900	0.17	0.44	12.2%	
		BBW = 100	104065	0.11	0.51	14.3%	
		BBW = 120	112762	0.09	0.52	12.7%	
		BBW = 140	118752	0.06	0.54	13.6%	
		BBW = 160	116494	0.11	0.49	20.3%	
		BBW = 180	132568	0.03	0.59	14.5%	
		BBW = 200	142590	0.03	0.62	15.4%	
SEED-BDT	$Qp = CC \cdot BBW^{a} \cdot SS^{b}$	BDT = 0.5	18400	0.44	0.19	21.4%	21.4%
		BDT = 1.0	19269	0.41	0.31	15.0%	
		BDT = 1.5	20323	0.35	0.28	14. 8%	
		BDT = 2.0	20589	0.31	0.27	15.1%	
		BDT = 2.5	19275	0.29	0.22	15.0%	
		BDT = 3.0	17907	0.28	0.19	15.6%	
		BDT = 3.5	16741	0.27	0.15	15.7%	
		BDT = 4.0	15109	0.27	0.11	16.7%	
		BDT = 4.5	13,742	0.27	0.07	17.9%	
		BDT = 5.0	12,206	0.28	0.04	18.3%	
SEED-SS	$Qp = CC \cdot \frac{BBW^{a}}{BDT^{b}}$	SS = 0.4	12,854	0.41	0.44	25.1%	25.1%
		SS = 0.6	17,010	0.37	0.49	22.4%	
		SS = 0.8	23,859	0.31	0.51	21.7%	
		SS = 1.0	30,695	0.27	0.52	21.7%	

* Maximum values for each equation are marked with bold letters

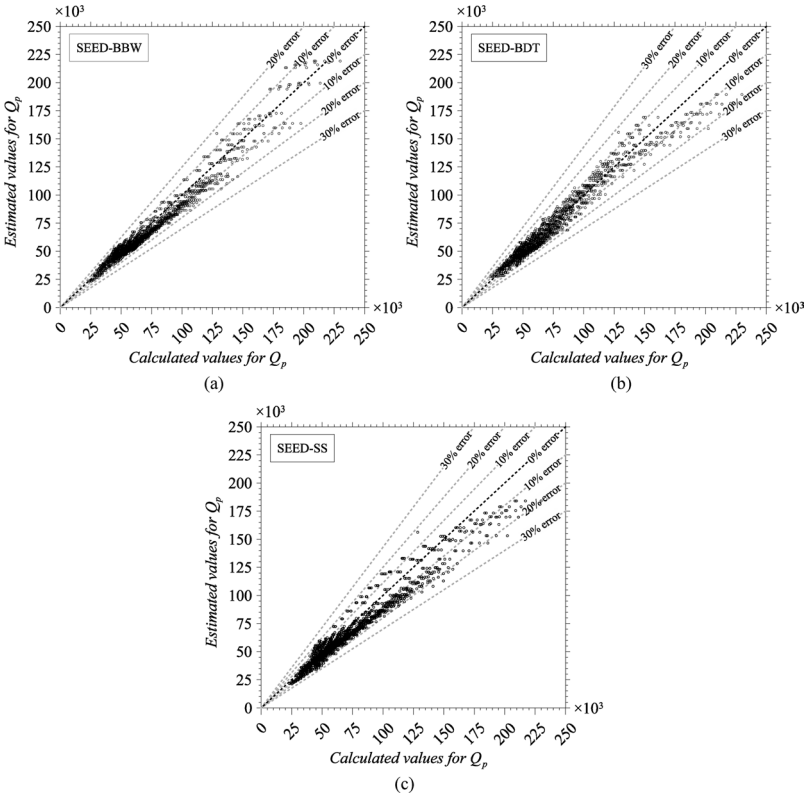


Fig. 11 Scatter plots of table-driven empirical equations

on piping-type breaches. The methodology presented in this study is designed to estimate peak discharge from earth-fill dam failures, with a particular focus on piping-type breaches. This approach's strength lies in its reliance on a large, robust synthetic dataset generated from 2,000 HEC-RAS simulations. This dataset provides a comprehensive foundation for deriving the model's coefficients through a meta-heuristic optimization algorithm (TLBO). The proposed table-driven empirical equations demonstrate a significant improvement in accuracy by adapting coefficients based on the value of a third parameter. This discussion aims to contextualize these findings by comparing our approach and results with those in the broader literature on dam breach analysis, as represented by the work of Wang et al. (2018), Xu and Zhang (2009), and Zhong et al. (2020). A key distinguishing factor of our study is our methodological choice to generate a synthetic dataset instead of relying on historical dam failure databases. Traditional empirical models, such as those developed by Wang et al. (2018), Xu and Zhang (2009), and Zhong et al. (2020), are derived from regression analyses of documented dam failure cases. While these historical datasets are invaluable, they are often limited by data scarcity, inconsistent measurements, and incomplete parameter reporting, as acknowledged by Wahl (1998) and implicitly addressed in these studies. For example, Wang et al. (2018) based their analysis on a database of 40 historical failures, whereas Xu and Zhang (2009) and Zhong et al. (2020) compiled larger databases of 75 and 162 cases respectively to enhance statistical robustness.

Our approach, centered on the Teton Dam case study, overcomes these limitations by generating a controlled, comprehensive dataset. This enables a systematic exploration of the parameter space (*BBW*, *BDT*, *SS*, H_w, and V_w, as well as their interactions), which would be nearly impossible with sparse and often incomplete historical records. However, this strength is also a limitation. The resulting SEED models are highly calibrated for piping failures in zoned earth-fill dams under conditions similar to those of the Teton Dam.

4 Conclusion

In this study, a novel family of simplified empirical equations was developed to estimate the peak discharge (Q_p) resulting from earth-fill dam failures, using key breach parameters including bottom breach width (*BBW*), breach development time (*BDT*), breach side slope (*SS*), water height at piping initiation (H_w), and volume of water above the breach invert (V_w). The effect of *BBW*, *SS*, *BDT*, H_w, and V_w parameters were investigated. A total of 2000 dam break scenarios were simulated in HEC-RAS under piping failure conditions, and the simulation results were used to analyze parameter sensitivity and determine empirical model coefficients using meta-heuristic optimization.

Based on the findings, the following conclusions are drawn:

- It is identified that *BBW* and *BDT* are sensitive parameters in dam break analysis. Satisfactory results can only be achieved with equations that include these two parameters.
- The *SS* parameter has a slight effect on the peak values of dam breach scenarios.
- H_w and V_w, while physically important, exhibit a nonlinear and *BDT*-dependent relationship with Q_p. They influence peak discharge in complex ways—such as increasing Q_p at lower H_w values for short *BDT*, but reducing it at higher H_w or longer *BDT*. Because their effects are non-monotonic and difficult to capture in a simplified empirical structure, they were not retained in the final equations. This should not be interpreted as their lack of physical importance, but rather as a modeling trade-off to achieve robust and simplified empirical formulations.
- Therefore, empirical equations based on *BBW, BDT,* and *SS* are derived. The results of the empirical equation developed herein are in good agreement with the simulated data obtained by HEC-RAS (12–25% error rate in Table 5).
- Within the scope of the study, single-parameter equations were also derived and analyzed, but it was observed that single-parameter models have relatively high error rates (80%). In addition, these models can produce values within a limited range and are insufficient to estimate high flow values. Therefore, it can be concluded that single-parameter models cannot be useful enough for peak discharge estimation.
- Compared to a single empirical equation with constant coefficients, the table-driven equation approach provides a better fit and more flexibility in representing the nonlinear effects of the parameters on peak flowrate. It effectively captured nonlinear interactions and significantly reduced the maximum error (20.3%–25.1%) compared to fixed-coefficient models.
- The results of the empirical equations named SEED-PII-1, SEED-PIII, SEED-BBW, SEED-BDT, and SEED-SS are in good agreement with the simulated data obtained by HEC-RAS software.

- In conclusion, the proposed SEED model provides a flexible framework capable of accommodating real-world dam breach behavior, especially under piping-type failure and time-critical conditions. However, users should remain aware that its applicability is primarily valid within the boundary conditions and failure mechanisms modeled — particularly those reflecting piping failures. For broader application across dam types and breach modes, further extensions and validations are recommended.
- Future research may focus on extending the applicability of the SEED model beyond piping-type failures in earth-fill dams to include other dam types (e.g., concrete and rock-fill dams) and different breach mechanisms such as overtopping and slope instability. Additional validation with real-world dam failure case studies from diverse geographical and climatic settings would further improve the reliability of the model. Moreover, the integration of the SEED equations into early warning and decision-support systems could enhance their practical use for dam safety management.

Supplementary Information The online version contains supplementary material available at https://doi.org/10.1007/s11269-025-04368-3.

Author Contributions All authors contributed to the study conception and design. Conceptualization and methodology were carried out by Rasim Temür, Yasin Paşa, and Sezar Gülbaz. Investigation was conducted by Yasin Paşa and İsmail Bilal Peker. Data curation was performed by Yasin Paşa and Sezar Gülbaz, while numerical analyses were carried out by Yasin Paşa and Abdülbaki Hacı. Coding and optimization procedures were performed by Rasim Temür. Visualization was completed by Rasim Temür, Yasin Paşa, and Sezar Gülbaz. The original draft of the manuscript was written by Rasim Temür, Sezar Gülbaz, and İsmail Bilal Peker. All authors contributed to the review and editing of the manuscript and approved the final version.

Funding Open access funding provided by the Scientific and Technological Research Council of Türkiye (TÜBİTAK). The authors declare that no funds, grants, or other support were received during the preparation of this manuscript.

Data and Code Availability The codes that support this study are available from the corresponding author upon request. The dataset used to develop the equations in the study is presented in the supplementary file.

Declarations

Ethical Approval All authors have read, understood, and have complied as applicable with the statements on "Duties of Authors" as found in the Guide for Authors.

Competing Interest The authors have no relevant financial or non-financial interests to disclose.

Open Access This article is licensed under a Creative Commons Attribution 4.0 International License, which permits use, sharing, adaptation, distribution and reproduction in any medium or format, as long as you give appropriate credit to the original author(s) and the source, provide a link to the Creative Commons licence, and indicate if changes were made. The images or other third party material in this article are included in the article's Creative Commons licence, unless indicated otherwise in a credit line to the material. If material is not included in the article's Creative Commons licence and your intended use is not permitted by statutory regulation or exceeds the permitted use, you will need to obtain permission directly from the copyright holder. To view a copy of this licence, visit http://creativecommons.org/licenses/by/4.0/.

References

Altinbilek D (2002) The role of dams in development. Int J Water Resour Dev 18(1):9–24. https://doi.org/10.1080/07900620220121620

Azmi M, Thomson K (2024) Dam breach parameters: from data-driven-based estimates to 2-dimensional modeling. Nat Hazards 120(5):4423–4461. https://doi.org/10.1007/s11069-023-06382-3
Baird IG, Ziegler AD, Fearnsid PM, Pineda A, Sasges G, Strube J, Thomas KA, Schmutz S, Greimel F, Hayes DS (2024) Ruin-of-the-rivers? A global review of run-of-the-river dams. Environ Manage 75:175–190. https://doi.org/10.1007/s00267-024-02062-5
Barnes MJ (1992) Famous failures revisiting major dam catastrophes. ASDSO Annual Conference. Baltimore. Association of State Dam Safety Officials
Bharath A, Shivapur AV, Hiremath CG, Maddamsetty R (2021) Dam break analysis using HEC-RAS and HEC-GeoRAS: a case study of Hidkal dam, Karnataka state, India. Environ Challenges 5:100401. https://doi.org/10.1016/j.envc.2021.100401
Brunner G (2014) Using HEC-RAS for dam break studies. U.S. Army Corps of Engineers, Hydrologic Engineering Center. TD-39. 609 Second Street, Davis, CA
Chadwick WL, Casagrande A, Coombs HA, Dowd MW, Fucik EM, Higginson RK, Leps TM, Peck RB, Seed HB, Jansen RB (1976) Failure of Teton Dam, Report to U.S Department of the Interior and State of Idaho, Idaho Falls, Idaho
Chen J, Shi H, Sivakumar B, Peart MR (2015) Population, water, food, energy and dams. Renewable Sustainable Energy Rev 56:18–28. https://doi.org/10.1016/j.rser.2015.11.043
Costa JE (1985) Floods from dam failures. United States Department of the Interior, Geological Survey. Open-File Report 85–560. Denver, CO
Costa JE, Schuster RL (1988) The formation and failure of natural dams. Geol Soc Am Bull 100(7):1054–1068. https://doi.org/10.3133/ofr87392
Dai S, Wang Y, Guo J, Song R, Shi Z, Yang S, Zhang Z, Zhang K, Liu H, Jin S (2025) Numerical simulation of dynamic process of dam-break flood and its impact on downstream dam surface. Water Resour Manage 39:4361–4391. https://doi.org/10.1007/s11269-025-04159-w
DHI (Danish Hydraulic Institute) (2017) A modelling system for rivers and channels (MIKE11), User Guide Manual. DHI water and environment. Denmark
Dhiman S, Patra KC (2019) Studies of dam disaster in India and equations for breach parameter. Nat Hazards 98(2):783–807. https://doi.org/10.1007/s11069-019-03731-z
Esri (2025a) Light gray canvas reference [basemap]. May 2, 2025. https://www.arcgis.com/home/item.html?id=1768e8369a214dfab4e2167d5c5f2454. Accessed 16 May 2025
Esri (2025b) World ocean base [basemap]. April 11, 2025. https://esri.maps.arcgis.com/home/item.html?id=1e126e7520f9466c9ca28b8f28b5e500. Accessed 16 May 2025
Esri (2025c) World imagery [basemap]. April 11, 2025. https://www.arcgis.com/home/item.html?id=10df2279f9684e4a9f6a7f08febac2a9. Accessed 16 May 2025
Evans SG (1986) The maximum discharge of outburst floods caused by the breaching of man-made and natural dams. Can Geotech J 23(3):385–387. https://doi.org/10.1139/t86-053
Fluixá-Sanmartín J, Altarejos-García L, Morales-Torres A, Escuder-Bueno I (2018) Review article: climate change impacts on dam safety. Nat Hazards Earth Syst Sci 18(9):2471–2488. https://doi.org/10.5194/nhess-18-2471-2018
Foster M, Fell R, Spannagle M (2000) The statistics of embankment dam failures and accidents. Can Geotech J 37(5):1000–1024. https://doi.org/10.1139/t00-030
Fread DL (1984) DAMBRK: The NWSS dam break flood forecasting model (4th ed.). Hydrologic Research Laboratory, National Weather Service, NOAA. National Weather Service (NWS) Report, NOAA, Silver Spring, MA
Froehlich DC (1995a) Embankment dam breach parameters revisited. First International Conference, Water Resources Engineering, Environmental and Water Resources Institute (EWRI). 14–18 August 1995. ASCE, Water Resources Engineering Proceeding, pp 887–891
Froehlich DC (1995b) Peak outflow from breached embankment dam. J Water Resour Plann Manage 121(1):90–97. https://doi.org/10.1061/(ASCE)0733-9496(1995)121:1(90)
Froehlich DC (2008) Embankment dam breach parameters and their uncertainties. J Hydraul Eng 134(12):1708–1721. https://doi.org/10.1061/(ASCE)0733-9429(2008)134:12(1708)
Galoie M, Zenz G, Eslamian S, Motamedi A (2012) Numerical simulation of flood due to dam-break flow using an implicit method. Int J Hydrol Sci Technol 2(2):117–137. https://doi.org/10.1504/ijhst.2012.047429
Ge W, Jiao Y, Wu M, Li Z, Wang T, Li W, Zhang Y, Gao W, Van Gelder P (2022) Estimating loss of life caused by dam breaches based on the simulation of floods routing and evacuation potential of population at risk. J Hydrol 612:128059. https://doi.org/10.1016/j.jhydrol.2022.128059
Gesch D, Oimoen M, Greenlee S, Nelson C, Steuck M, Tyler D (2002) The national elevation dataset. Photogramm Eng Remote Sens 68(1):5–32
Google Earth Pro (2025) http://www.google.com/earth/index.html. Accessed 31 May 2025
Graham W (2008) The Teton Dam failure: An effective warning and evacuation. ASDSO Annual Conference. Indian Wells Association of State Dam Safety Officials

Gulbaz S, Kazezyılmaz-Alhan CM, Temür R (2019) Development of an empirical formula for estimation of bioretention outflow rate. Water SA 45. https://doi.org/10.4314/wsa.v45i2.07

Hagen VK (1982) Re-evaluation of design floods and dam safety. Proceedings of 14th ICOLD Congress, Rio De Janeiro, Brazil. 1, pp 475–491

Haltas I, Tayfur G, Elci S (2016) Two-dimensional numerical modeling of flood wave propagation in an urban area due to Ürkmez dam-break, İzmir, Turkey. Nat Hazards 81:2103–2119. https://doi.org/10.1007/s11069-016-2175-6

He G, Chai J, Qin Y, Xu Z, Li S (2020) Evaluation of dam break social impact assessments based on an improved variable fuzzy set model. Water 12(4):970. https://doi.org/10.3390/w12040970

Hooshyaripor F, Tahershamsi A (2015) Effect of reservoir side slopes on dam-break flood waves. Eng Appl Comput Fluid Mech 9(1):458–468. https://doi.org/10.1080/19942060.2015.1039630

Kirkpatrick GW (1977) Evaluation guidelines for spillway adequacy, the evaluation of dam safety. Engineering Foundation Conference, ASCE, New York, pp 395–414

Kumar S, Jaswal A, Pandey A, Sharma N (2017) Literature review of dam break studies and inundation mapping using hydraulic models and GIS. IJRET 4(5):55–61

Liu Y, Zhang X, Sun Y, Yu H, Sun C, Li Z, Li X (2024) Characterization of partial dam-break waves: effects of upstream and downstream water levels. Water Resour Manage 39(2):759–777. https://doi.org/10.1007/s11269-024-03989-4

Lyu Z, Chai J, Xu Z, Qin Y, Cao J (2019) A comprehensive review on reasons for tailings dam failures based on case history. Adv Civ Eng 2019:159306. https://doi.org/10.1155/2019/4159306

Macchione F, Costabile P, Costanzo C, De Lorenzo G, Razdar B (2015) Dam breach modelling: influence on downstream water levels and a proposal of a physically based module for flood propagation software. J Hydroinf 18(4):615–633. https://doi.org/10.2166/hydro.2015.250

MacDonald Thomas C, Langridge-Monopolis J (1984) Breaching characteristics of dam failures. J Hydraul Eng 110(5):567–586. https://doi.org/10.1061/(ASCE)0733-9429(1984)110:5(567)

Marangoz HO, Anılan T, Karasu S (2024) Investigating the non-linear effects of breach parameters on a dam break study. Water Resour Manage 38(5):1773–1790. https://doi.org/10.1007/s11269-024-03765-4

Moreno-Rodenas A, Mantilla-Jones JD, Valero D (2025) Age, climate and economic disparities drive the current state of global dam safety. Nat Water 3:284–295. https://doi.org/10.1038/s44221-025-00402-1

Nasser R, Tzioutzios D, Liu Y (2025) Statistical analysis of global dam accidents in the 21st century: a focus on common features and causes. Water Resour Manage. https://doi.org/10.1007/s11269-025-04259-7

Paşa Y, Peker İB, Hacı A, Gülbaz S (2023) Dam failure analysis and flood disaster simulation under various scenarios. Water Sci Technol 87(5):1214–1231. https://doi.org/10.2166/wst.2023.052

Peng M, Zhang LM (2013) Dynamic decision making for dam-break emergency management – Part 1: theoretical framework. Nat Hazards Earth Syst Sci 13(2):425–437. https://doi.org/10.5194/nhess-13-425-2013

Peng J, Zhang J, Sayama T (2024) Assessment of loss of life owing to dam-failure flooding considering population distribution and evacuation. Int J Disaster Risk Reduct 112:104737. https://doi.org/10.1016/j.ijdrr.2024.104737

Qiu W, Li Y, Zhao W, Zhang Q, Wen L, Zhang Y, Wang T (2024) Mathematical model and application of overtopping breach of cascade earth-rock dams considering flood peak enhancement effect. Water Resour Manage 39:1403–1433. https://doi.org/10.1007/s11269-024-04022-4

Rao R, Savsani V, Vakharia D (2011) Teaching–learning-based optimization: a novel method for constrained mechanical design optimization problems. Comput-Aided Des 43(3):303–315. https://doi.org/10.1016/j.cad.2010.12.015

Sanchez-Mondragon J, Fontes JVH, Espinoza-Haro MP, Esperança PTT (2023) Interaction of wet dam-break flows with a structure: on the effects of surface tension and gate opening velocity in water surface evolution using MPS method. Comput Part Mech 10(5):1221–1244. https://doi.org/10.1007/s40571-023-00561-6

SCS (1981) Simplified dam-breach routing procedure. United States Department of Agriculture, Soil Conservation Service (SCS), Technical Release No. 66 (Rev. 1), 39

Shourian M, Mousavi SJ, Tahershamsi A (2007) Basin-wide water resources planning by integrating PSO algorithm and MODSIM. Water Resour Manage 22(10):1347–1366. https://doi.org/10.1007/s11269-007-9229-1

Singh KP, Snorrason A (1984) Sensitivity of outflow peaks and flood stages to the selection of dam breach parameters and simulation models. J Hydrol 68(1–4):295–310. https://doi.org/10.1016/0022-1694(84)90217-8

Snorteland N (2009) Fontenelle Dam, Ririe Dam, and Teton Dam: An examination of the influence of organizational culture on decision-making. ASDSO Annual Conference, Hollywood. Association of State Dam Safety Officials

Stamou AI, Mitsopoulos G, Sfetsos A, Stamou AT, Sideris S, Varotsos KV, Giannakopoulos C, Koutroulis A (2025) Vulnerability assessment of dams and reservoirs to climate change in the Mediterranean region: the case of the Almopeos Dam in northern Greece. Water 17(9):1289. https://doi.org/10.3390/w17091289

USACE (2016) HEC-RAS River Analysis System, 2D Modeling User's Manual Version 5.0; US Army Corps of Engineers California USA: Davis, CA, USA
USACE (2020) HEC-RAS river analysis system hydraulic reference manual, pg. 345, December 2020, US Army Corps of Engineers California USA: Davis, CA, USA. 95616
USBR (1982) Guidelines for defining inundated areas downstream from Bureau of Reclamation dams. Reclamation Planning Instruction, 82–11; 15 June 1982, U.S. Bureau of Reclamation
Von Thun JL, Gillette DR (1990) Guidance on breach parameters. Unpublished internal document, U.S. Bureau of Reclamation, Denver, CO, 17, March 1990
Wahl TL (1998) Prediction of embankment dam breach parameters–A literature review and needs assessment. DSO-98–004, Dam Safety Research Report. U.S. Department of the Interior Bureau of Reclamation, Dam Safety Office (DSO), Water Resources Research Laboratory
Walder JS, O'Connor JE (1997) Methods for predicting peak discharge of floods caused by failure of natural and constructed earthen dams. Water Resour Res 33(10):2337–2348. https://doi.org/10.1029/97wr01616
Wang B, Chen Y, Wu C, Peng Y, Song J, Liu W, Liu X (2018) Empirica and semi analytical models for predicting peak outflow caused by embankment dam failures. J Hydrol 692–702. https://doi.org/10.1016/j.jhydrol.2018.05.049
Wang Y, Fu Z, Cheng Z, Xiang Y, Chen J, Zhang P, Yang X (2024) Uncertainty analysis of dam-break flood risk consequences under the influence of non-structural measures. Int J Disaster Risk Reduct 102:104265. https://doi.org/10.1016/j.ijdrr.2024.104265
Xiong Y (2011) A dam break analysis using HEC-RAS. J Water Resour Prot 3(6):370–379. https://doi.org/10.4236/jwarp.2011.36047
Xu Y, Zhang LM (2009) Breaching parameters for earth and rockfill dams. J Geotech Geoenviron Eng 135(12):1957–1970. https://doi.org/10.1061/(asce)gt.1943-5606.0000162
Xu F, Zhou H, Zhou J, Yang X (2012) A mathematical model for forecasting the dam-break flood routing process of a landslide dam. Math Probl Eng 2012:139642. https://doi.org/10.1155/2012/139642
Zamarrón-Mieza I, Yepes V, Moreno-Jiménez JM (2017) A systematic review of application of multi-criteria decision analysis for aging-dam management. J Cleaner Prod 147:217–230. https://doi.org/10.1016/j.jclepro.2017.01.092
Zhang Y, Li Z, Wang J, Ge W, Chen X (2022a) Environmental impact assessment of dam-break floods considering multiple influencing factors. Sci Total Environ 837:155853. https://doi.org/10.1016/j.scitotenv.2022.155853
Zhang X, Wang CY, Wong H, Jiang T, Dong J (2022b) Modeling dam deformation in the early stage of internal seepage erosion–application to the Teton Dam, Idaho, before the 1976 incident. J Hydrol 605:127378. https://doi.org/10.1016/j.jhydrol.2021.127378
Zhong Q, Chen S, Fu Z, Shan Y (2020) New empirical model for breaching of earth-rock dams. Nat Hazard Rev 21(2):06020002. https://doi.org/10.1061/(asce)nh.1527-6996.0000374
Zhu X, Bao T, Yeoh JKW, Jia N, Li H (2021) Enhancing dam safety evaluation using dam digital twins. Struct Infrastruct Eng 19(7):904–920. https://doi.org/10.1080/15732479.2021.1991387

Publisher's Note Springer Nature remains neutral with regard to jurisdictional claims in published maps and institutional affiliations.

Authors and Affiliations

Rasim Temür[1] · Yasin Paşa[2] · Sezar Gülbaz[3] · İsmail Bilal Peker[3] · Abdülbaki Hacı[2]

✉ Rasim Temür
temur@iuc.edu.tr

[1] Department of Civil Engineering, Mechanics Division, İstanbul University-Cerrahpaşa, Istanbul, Turkey

[2] Department of Civil Engineering, İstanbul Gelişim University, Istanbul, Turkey

[3] Department of Civil Engineering, Hydraulics Division, İstanbul University-Cerrahpaşa, Istanbul, Turkey